Angular dependence of the tunneling anisotropic magnetoresistance in magnetic tunnel junctions

A. Matos-Abiague, M. Gmitra, and J. Fabian
Institute for Theoretical Physics, University of Regensburg, 93040 Regensburg, Germany
(Received 14 April 2009; revised manuscript received 22 June 2009; published 16 July 2009)

Based on general symmetry considerations, we investigate how the dependence of the tunneling anisotropic magnetoresistance (TAMR) on the magnetization direction is determined by the specific form of the spin-orbit coupling field. By extending a phenomenological model, previously proposed for explaining the main trends of the TAMR in (001) ferromagnet/semiconductor/normal-metal magnetic tunnel junctions (MTJs) [J. Moser *et al.*, Phys. Rev. Lett. **99**, 056601 (2007)], we provide a unified qualitative description of the TAMR in MTJs with different growth directions. In particular, we predict the forms of angular dependences of the TAMR in (001), (110), and (111) MTJs with structure inversion asymmetries and/or bulk inversion asymmetries. The effects of in-plane uniaxial strain on the TAMR are also investigated.

DOI: 10.1103/PhysRevB.80.045312 PACS number(s): 73.43.Jn, 72.25.Dc, 73.43.Qt

I. INTRODUCTION

The tunneling anisotropic magnetoresistance (TAMR) effect refers to the dependence of the magnetoresistance of magnetic tunnel junctions (MTJs) on the absolute orientation(s) of the magnetization(s) in the ferromagnetic lead(s) with respect to the crystallographic axes.[1–4] Unlike the conventional tunneling magnetoresistance (TMR) effect, the TAMR is not only present in MTJs in which both electrodes are ferromagnetic but may also appear in tunneling structures with a single magnetic electrode.[1,5] Because of this remarkable property, if the major challenge of increasing the size of the effect at room temperature is solved, the TAMR could be an attractive candidate for applications in the design of new spin-valve-based devices whose components could operate with a single magnetic lead. In what follows we focus our discussion on the case of MTJs in which only one of the electrodes is ferromagnetic.

The TAMR has been experimentally and theoretically investigated in a variety of systems under different configurations.[1–19] This diversity has made it difficult to build a unified theory of the TAMR. In fact, although there exists a general consensus in identifying the spin-orbit coupling (SOC) as the mechanism responsible for the TAMR, it has been recognized that the way the SOC influences the TAMR may depend on the considered system and configuration.

Two different configurations, the *in-plane* and *out-of-plane* configurations, have been considered for investigating the TAMR (for an extensive discussion see Ref. 19 and references therein). The in-plane TAMR refers to the changes in the tunneling magnetoresistance when the magnetization direction, defined with respect to a fixed reference axis $[x]$, is rotated in the plane of the ferromagnetic layer. The in-plane TAMR ratio is defined as[19]

$$\mathrm{TAMR}^{\mathrm{in}}_{[x]}(\phi) = \frac{R(\theta=90°,\phi) - R(\theta=90°,\ \phi=0)}{R(\theta=90°,\ \phi=0)}, \quad (1)$$

where $R(\theta,\phi)$ denotes the tunneling magnetoresistance for the magnetization oriented along the direction defined by the unit vector $\hat{\mathbf{m}}=(\sin\theta\cos\phi,\sin\theta\sin\phi,\cos\theta)$ (see Fig. 1).

In the out-of-plane configuration, the TAMR measures the changes in the tunneling magnetoresistance, when the magnetization is rotated within the plane defined by the reference axis $[x]$ and the direction normal to the ferromagnetic layer. The out-of-plane TAMR is given by[19]

$$\mathrm{TAMR}^{\mathrm{out}}_{[x]}(\theta) = \frac{R(\theta,\phi=0) - R(\theta=0,\ \phi=0)}{R(\theta=0,\ \phi=0)}. \quad (2)$$

An important property of the TAMR is the form of its angular dependence. It has been experimentally shown that both the in-plane and out-of-plane TAMR exhibit a rather regular and relatively simple angular dependence with a well-defined symmetry, in spite of the highly complicated band structure of the considered systems.[4,5,11,17] This suggests that although the size of the TAMR may depend on the detailed band structure of the system, its angular dependence is essentially determined by the symmetry properties of the SOC field. Here we investigate how the specific form of the TAMR angular dependence emerges from the properties of the SOC field.

A phenomenological model, which incorporates the effects of the interference of Bychkov-Rashba and Dresselhaus SOCs was recently developed to explain the in-plane TAMR in (001) ferromagnet/semiconductor/normal-metal MTJs.[5,12,19] In particular, it was shown that, in spite of its relative simplicity, the model was able to reproduce the two-

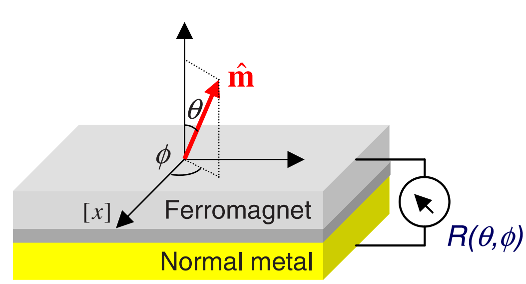

FIG. 1. (Color online) Schematic of a MTJ composed of a normal-metal lead (bottom layer), a semiconductor or insulator barrier (central layer), and a ferromagnetic electrode (top layer). The vector $\hat{\mathbf{m}}$ indicates the magnetization orientation, while $[x]$ denotes a reference crystallographic axis.

fold symmetric angular dependence of the in-plane TAMR experimentally observed in (001) Fe/GaAs/Au MTJs.[5,12] In such heterojunctions all the involved materials are cubic in their bulk forms. Therefore, the twofold anisotropy of the in-plane TAMR must originate from the interfaces. Here we generalize the model and provide a unified qualitative description of the angular dependence of both the in-plane and out-of-plane TAMRs in (001), (110), and (111) MTJs. We consider systems in which the SOC originates from structure inversion asymmetry (SIA) (Bychkov-Rashba-type SOC) and/or bulk inversion asymmetry (BIA) (Dresselhaus-type SOC) and predict different forms of the TAMR angular dependence which could be tested in future experiments. The effects of uniaxial strain are also discussed.

II. THEORETICAL MODEL

We consider a MTJ composed of a ferromagnetic electrode and a normal-metal counter electrode separated by an insulator or a semiconductor barrier. However, our conclusions are also valid for the case of MTJs with two ferromagnetic electrodes, whose magnetizations are parallel to each other, since such systems are qualitatively similar to the case of MTJs with a single ferromagnetic lead.

The z direction is fixed along the normal to the ferromagnetic layer (i.e., parallel to the growth direction). The effective spin-orbit interaction corresponding to the nth band can be written as

$$H_{\mathrm{SO}} = \mathbf{w}_n(\mathbf{k}) \cdot \boldsymbol{\sigma}, \tag{3}$$

where $\mathbf{w}_n(\mathbf{k})=[w_{nx}(\mathbf{k}),w_{ny}(\mathbf{k}),w_{nz}(\mathbf{k})]$ is the effective SOC field associated to the nth band, $\mathbf{k}$ is the wave vector, and $\boldsymbol{\sigma}$ is the vector whose components are the Pauli matrices. Equation (3) is quite general, since by now we have not considered any specific form for the SOC field. The detailed form of the SOC field can be quite complicated as one goes away from the center of the Brillouin zone and quite different from band to band, as recently demonstrated by first-principles calculations.[20]

Due to the presence of the spin-orbit interaction, the transmissivity $T_n(\mathbf{k},\hat{\mathbf{m}})$ corresponding to the nth band becomes dependent on the magnetization direction $\hat{\mathbf{m}}$. Assuming that the strength of the SOC field is small relative to both the Fermi energy and the exchange splitting, one can expand the transmissivity in powers of $\mathbf{w}_n(\mathbf{k})$. For a given n and $\mathbf{k}$ there are only two preferential directions in the system, defined by $\hat{\mathbf{m}}$ and $\mathbf{w}_n$. Since the transmissivity is a scalar function, it can be written, to second order in the SOC field strength, in the form[5,12,19]

$$T_n(\mathbf{k},\hat{\mathbf{m}}) \approx a_{1n}^{(0)}(\mathbf{k}) + a_{1n}^{(1)}(\mathbf{k})[\hat{\mathbf{m}}\cdot\mathbf{w}_n(\mathbf{k})] + a_{1n}^{(2)}(\mathbf{k})|\mathbf{w}_n(\mathbf{k})|^2 + a_{2n}^{(2)}(\mathbf{k})[\hat{\mathbf{m}}\cdot\mathbf{w}_n(\mathbf{k})]^2, \tag{4}$$

which represents the most general expansion (up to second order) of a scalar function (the transmissivity) in terms of two vectors ($\hat{\mathbf{m}}$ and $\mathbf{w}_n$). Note that the arguments used for obtaining Eq. (4) are also valid for MTJs with two ferromagnetic electrodes, whose magnetizations are parallel to each other along the direction $\hat{\mathbf{m}}$. The expansion coefficients, $a_{in}^{(j)}(i=1,2;\ j=0,1,2)$, refer to the system in the absence of the SOC field, and therefore, do not depend on $\hat{\mathbf{m}}$. Since these coefficients reflect the cubic symmetry of the involved bulk materials, they obey the relations $a_{in}^{(j)}(k_x,k_y)=a_{in}^{(j)}(-k_x,-k_y)$, $a_{in}^{(j)}(k_x,k_y)=a_{in}^{(j)}(-k_x,k_y)$, and $a_{in}^{(j)}(k_x,k_y)=a_{in}^{(j)}(k_y,k_x)$. Cases in which the involved materials have other than cubic symmetries in their bulk form can be treated analogously.

Within linear-response theory, the conductance G through the MTJ is determined by the states at the Fermi energy E_F. In such a case $k_z=k_z(E_F,\mathbf{k}_\parallel)$ and the $\mathbf{k}$ dependence of the transmissivity reduces to the in-plane $\mathbf{k}_\parallel$ dependence at $E=E_F$. One can then write

$$G(\hat{\mathbf{m}}) = \frac{e^2}{(2\pi)^3 h}\sum_n \int d^2\mathbf{k}_\parallel T_n(\mathbf{k}_\parallel,\hat{\mathbf{m}}) = \frac{g_0}{8\pi^2}\sum_n \langle T_n(\mathbf{k}_\parallel,\hat{\mathbf{m}})\rangle, \tag{5}$$

where $T_n(\mathbf{k}_\parallel,\hat{\mathbf{m}})$ is the transmissivity at $E=E_F$ and $g_0=2e^2/h$ is the conductance quantum. In Eq. (5) and in what follows, we use the simplified notation $\langle\cdots\rangle$ for the integration over $\mathbf{k}_\parallel$ on the Fermi surface.

The time-reversal symmetry implies that $T_n(\mathbf{k},\hat{\mathbf{m}})=T_n(-\mathbf{k},-\hat{\mathbf{m}})$ and $\mathbf{w}_n(\mathbf{k})=-\mathbf{w}_n(-\mathbf{k})$. It follows then from Eq. (4) that the first-order term in the expansion must be an odd function of $\mathbf{k}$ and will, therefore, vanish after integration over $\mathbf{k}_\parallel$. As a result the conductance can be rewritten as

$$G(\hat{\mathbf{m}}) = G^{(0)} + G_{\mathrm{iso}}^{(2)} + G_{\mathrm{aniso}}^{(2)}(\hat{\mathbf{m}}), \tag{6}$$

where $G^{(0)}$ is the conductance in the absence of SOC, $G_{\mathrm{iso}}^{(2)} \propto \langle a_{1n}^{(2)}(\mathbf{k}_\parallel)|\mathbf{w}_n(\mathbf{k}_\parallel)|^2\rangle$ and

$$G_{\mathrm{aniso}}^{(2)}(\hat{\mathbf{m}}) = \frac{g_0}{8\pi^2}\sum_n \langle a_{2n}^{(2)}(\mathbf{k}_\parallel)[\hat{\mathbf{m}}\cdot\mathbf{w}_n(\mathbf{k}_\parallel)]^2\rangle \tag{7}$$

are the isotropic and anisotropic SOC contributions, respectively. In terms of the components of $\hat{\mathbf{m}}$ and the SOC field, Eq. (7) reduces to

$$G_{\mathrm{aniso}}^{(2)}(\theta,\phi) = \frac{g_0}{8\pi^2}\mathrm{Tr}[AM(\theta,\phi)], \tag{8}$$

where A and $M(\theta,\phi)$ are matrices whose elements are given by

$$A_{ij} = \sum_n \langle a_{2n}^{(2)}(\mathbf{k}_\parallel)w_{ni}w_{nj}\rangle \quad (i,j=x,y,z) \tag{9}$$

and

$$M_{ij}(\theta,\phi) = m_i(\theta,\phi)m_j(\theta,\phi) \quad (i,j=x,y,z), \tag{10}$$

respectively.

Equations (8)–(10) are quite general and reveal how the symmetry of the SOC field can lead to the anisotropy of the conductance. Further simplifications of these expressions can be realized by taking into account the properties of the specific form of the SOC field. From the time-reversal symmetry it follows that the SOC field has to be an odd function of the wave vector. Thus in the lowest-order approximation with respect to $\mathbf{k}_\parallel$, the SOC field is linear in k_x and k_y. In this case, the most general form of the SOC field components is $w_{ni}=d_{ni}^x k_x+d_{ni}^y k_y=\mathbf{d}_{ni}\cdot\mathbf{k}_\parallel (i=x,y,z)$. As shown below, many relevant physical situations correspond to such a case. The matrix elements in Eq. (9) then reduce to

$$A_{ij} = \sum_n c_n(\mathbf{d}_{ni} \cdot \mathbf{d}_{nj}). \qquad (11)$$

In obtaining Eq. (11) we took into account the fourfold symmetry of the expansion coefficients $a^{(2)}_{2n}(\mathbf{k}_\parallel)$ from which follows that the only nonvanishing averages are of the form $c_n = \langle a^{(2)}_{2n}(\mathbf{k}_\parallel) k_x^2 \rangle = \langle a^{(2)}_{2n}(\mathbf{k}_\parallel) k_y^2 \rangle$. By using the Eqs. (8), (10), and (11) the anisotropic part of the conductance can be rewritten as

$$G^{(2)}_{\text{aniso}} = \frac{g_0}{8\pi^2} \sum_{i,j,n} c_n m_i(\theta,\phi) m_j(\theta,\phi)(\mathbf{d}_{ni} \cdot \mathbf{d}_{nj}). \qquad (12)$$

The dependence of the TAMR ratio on the magnetization direction is determined by the anisotropic part of the conductance. Thus, Eq. (12) is our starting formula for discussing important particular cases.

III. RESULTS

We first neglect the effects of strain and focus on the particularly relevant case in which the SOC field results from the interference of the Bychkov-Rashba and Dresselhaus SOCs. Later on we shall consider also MTJs with SOC induced by uniaxial strain.

The Bychkov-Rashba SOC originates from the structure inversion asymmetry of the junction and is basically determined by the strong electric fields at the interfaces of the tunneling barrier. It is present, for example, in MTJs with the left and right electrodes made of different materials, and therefore, with broken inversion symmetry. Since the interface electric field points along the growth (z) direction of the MTJ, the Bychkov-Rashba SOC has the form[21]

$$H_{\text{BR}} = \alpha(k_x\sigma_y - k_y\sigma_x), \qquad (13)$$

where the SOC parameter α is proportional to the average electric field. The Hamiltonian H_{BR} is invariant under rotations around the z axis. Therefore, as long as the z axis is chosen to point in the growth direction, the Bychkov-Rashba SOC has always the form given in Eq. (13), irrespective of the specific orientation of the crystallographic axes.

The Dresselhaus SOC results from the bulk inversion asymmetry of one or more of the constituent materials. Typical materials with BIA are the zinc-blende semiconductors. Thus, the Dresselhaus SOC can be relevant for MTJs with noncentrosymmetric semiconductor barriers. Unlike the Bychkov-Rashba SOC, the form of the Dresselhaus SOC (which emerges from the BIA of the crystal itself) depends on the orientation of the crystallographic axes. Therefore the specific form of the total SOC field depends on the growth direction of the heterostructure. The SOC Hamiltonians can be found from the theory of invariants[22,23] by constructing the most general Hamiltonian compatible with the crystal symmetries. Below we focus in the study of the most relevant cases, corresponding to MTJs grown in the [001], [110], and [111] crystallographic directions.

A. (001) MTJs with axes $\hat{\mathbf{x}}\|[110]$, $\hat{\mathbf{y}}\|[\bar{1}10]$, and $\hat{\mathbf{z}}\|[001]$

For a (001) noncentrosymmetric barrier with zinc-blende structure, the corresponding point group is D_{2d}. In such a case the Dresselhaus SOC which is compatible with this symmetry has the form (after linearization)[24,25]

$$H_{\text{D}} = -\gamma(k_x\sigma_y + k_y\sigma_x), \qquad (14)$$

where γ is a material parameter characterizing the SOC strength. At the interfaces, however, the different orientations of the bonds may lower the symmetry to C_{2v} with the twofold rotation axis C_2 along the growth direction [this is, for example, the case of an epitaxial (001) Fe/GaAs interface].[12] The C_{2v} symmetry accounts for the presence of both BIA and SIA. In such a case the SOC corresponding to the nth band contains both Bychkov-Rashba and Dresselhaus terms [see Eqs. (13) and (14), respectively] and is given by[12,21,24]

$$H_{\text{SO}} = (\alpha_n - \gamma_n)k_x\sigma_y - (\alpha_n + \gamma_n)k_y\sigma_x, \qquad (15)$$

where α_n and γ_n are the corresponding Bychkov-Rashba and Dresselhaus parameters, respectively.

One can extract the components of the SOC field by comparing Eqs. (3) and (15). It follows then from Eq. (12) that the angular dependence of the anisotropic conductance is given by

$$G^{(2)}_{\text{aniso}} = \frac{g_0 \sin^2\theta}{8\pi^2} \sum_n c_n[(\alpha_n^2 + \gamma_n^2) + 2\alpha_n\gamma_n\cos(2\phi)]. \qquad (16)$$

The expression above together with Eqs. (1) and (2) lead to the relations corresponding to case A in Table I.[26] The obtained TAMR coefficients, which are valid up to second order in the SOC field, reveal a clear distinction between the in-plane and out-of-plane configurations in [001] MTJs: while for a finite out-of-plane TAMR the presence of only one of the SOCs suffices (i.e., it is sufficient to have $\alpha_n \neq 0$ or $\gamma_n \neq 0$), the twofold symmetric in-plane TAMR appears because of the interference of nonvanishing Bychkov-Rashba and Dresselhaus SOCs (i.e., both α_n and γ_n have to be finite).[27] This explains why a finite out-of-plane TAMR appears in MTJs such as Fe(001)/vacuum/Cu(001) in which only the Bychkov-Rashba SOC is present.[10] It is also in agreement with the recent observation of the in-plane TAMR in epitaxial (001) Fe/GaAs/Au MTJs,[5] where, due to the presence of the noncentrosymmetric zinc-blende semiconductor (GaAs), not only the Bychkov-Rashba but also the Dresselhaus SOC become relevant. In both the in-plane and out-of-plane configurations, angular dependencies of the form $\text{TAMR}^{\text{in}}_{[110]}(\phi) \propto [1 - \cos(2\phi)]$ and $\text{TAMR}^{\text{out}}_{[110]}(\theta) \propto [\cos(2\theta) - 1]$ (see Table I) have been experimentally measured.[4,5,11,17]

The results displayed in Table I suggest the possibility of using different configurations and reference axes as complementary setups for TAMR measurements. In particular, our theoretical model predicts that in the regime $\alpha_n \approx \gamma_n$ the out-of-plane TAMR with reference axis in the $[\bar{1}10]$ is suppressed, while it remains finite if the complementary axis [110] is used as a reference.[28] The opposite behavior, i.e.,

TABLE I. TAMR coefficients in units of $g_0/[16\pi^2(G^{(0)}+G^{(2)}_{\text{iso}})]$ for different structures, reference axes $[x]$, and configurations.

Case	Structure	$[x]$	In-plane $\text{TAMR}^{\text{in}}_{[x]}(\phi)$	Out-of-plane $\text{TAMR}^{\text{out}}_{[x]}(\theta)$
A	(001) MTJ	[110]	$4[1-\cos(2\phi)]\Sigma_n c_n\alpha_n\gamma_n$	$[\cos(2\theta)-1]\Sigma_n c_n(\alpha_n+\gamma_n)^2$
		$[\bar{1}10]$	$4[\cos(2\phi)-1]\Sigma_n c_n\alpha_n\gamma_n$	$[\cos(2\theta)-1]\Sigma_n c_n(\alpha_n-\gamma_n)^2$
B	(110) MTJ	$[\bar{1}10]$	$[1-\cos(2\phi)]\Sigma_n c_n(\alpha_n^2-\beta_n^2)$	$[\cos(2\theta)-1]\Sigma_n c_n(\alpha_n^2-\lambda_n^2)$
		[001]	$[\cos(2\phi)-1]\Sigma_n c_n(\alpha_n^2-\beta_n^2)$	$2\Sigma_n c_n[\lambda_n^2-(\beta_n\sin\theta+\lambda_n\cos\theta)^2]$
C	(111) MTJ	$[11\bar{2}]$	0	$[\cos(2\theta)-1]\Sigma_n c_n(\alpha_n+\gamma_n)^2$
		$[\bar{1}10]$	0	$[\cos(2\theta)-1]\Sigma_n c_n(\alpha_n+\gamma_n)^2$
D	strained (001) MTJ	[110]	$4[1-\cos(2\phi)]\Sigma_n c_n\eta_n\mu_n$	$[\cos(2\theta)-1]\Sigma_n c_n(\eta_n+\mu_n)^2$
		$[\bar{1}10]$	$4[\cos(2\phi)-1]\Sigma_n c_n\eta_n\mu_n$	$[\cos(2\theta)-1]\Sigma_n c_n(\eta_n-\mu_n)^2$

$\text{TAMR}^{\text{out}}_{[\bar{1}10]}\neq 0$ and $\text{TAMR}^{\text{out}}_{[110]}=0$, is expected when $\alpha_n\approx -\gamma_n$. Another relevant regime occurs when $\alpha_n\approx 0$, for which the in-plane TAMR is expected to vanish (see case A in Table I). The existence of such a regime was previously invoked in Refs. 5 and 12 for explaining the suppression of the in-plane TAMR experimentally observed in (001) Fe/GaAs/Au MTJs.[5] Our theory predicts that although the in-plane TAMR vanishes, the out-of-plane TAMR should remain finite in such a regime. In fact, in the regime $\alpha_n\approx 0$ the amplitude of the out-of-plane TAMR constitutes a direct measurement of the effects of BIA in the noncentrosymmetric barrier.

By combining the results shown in Table I one can find expressions such as

$$\text{TAMR}^{\text{in}}_{[110]}(90°)=\text{TAMR}^{\text{out}}_{[\bar{1}10]}(90°)-\text{TAMR}^{\text{out}}_{[110]}(90°), \tag{17}$$

which correlates the in-plane and out-of-plane TAMR coefficients and can be experimentally tested.

B. (110) MTJs with axes $\hat{x}\|[\bar{1}10]$, $\hat{y}\|[001]$, and $\hat{z}\|[110]$

In the case of a (110) zinc-blende barrier the symmetry group is C_{2v} with the twofold rotation axis lying in the plane perpendicular to the growth direction. The BIA-like SOC has the form[23]

$$H^{(110)}_{\text{BIA}}=\lambda k_x\sigma_z. \tag{18}$$

The presence of interfaces may result in SIA and can lower the symmetry to a single reflection plane. The SOC in the nth band can be written as[23,29]

$$H_{\text{SO}}=\beta_n k_x\sigma_y-\alpha_n k_y\sigma_x+\lambda_n k_x\sigma_z. \tag{19}$$

Here α_n and β_n are the parameters related to the SIA-induced SOC, while λ_n characterizes the strength of the SOC resulting from the BIA [see Eq. (18)]. Note that because of the reduced symmetry of the (110) structures with respect to the (001) MTJs, in the present case the usual SIA-induced SOC acquires, in addition to the usual Bychkov-Rashba SOC [see Eq. (13)], an extra contribution, which leads to $\alpha_n\neq\beta_n$ in Eq. (19).[23,29] Proceeding in the same way as in Sec. III A we obtain the following relation for the anisotropic contribution to the conductance

$$G^{(2)}_{\text{iso}}=\frac{g_0}{8\pi^2}\sum_n c_n[(\alpha_n^2\cos^2\phi+\beta_n^2\sin^2\phi)\sin^2\theta+\lambda_n^2\cos^2\theta + \beta_n\lambda_n\sin\phi\sin(2\theta)]. \tag{20}$$

The corresponding TAMR coefficients are given in Table I (case B). They show that the angular dependences of the TAMR in both the in-plane and out-of-plane configurations are similar to the ones obtained for the (001) MTJs [compare the cases A and B in Table I]. However, their physical origin is now different. In the present case the in-plane TAMR originates from the SIA-induced SOC while the out-of-plane TAMR has contributions arising from both SIA-like and BIA-like SOCs. Thus, our model predicts that in (110) MTJs it could be possible to observe the TAMR in the two configurations even if the tunneling barrier is composed of a centrosymmetric material. Another observation is that the out-of-plane TAMR with reference axis along the $[\bar{1}10]$ direction could be suppressed if under some given conditions the regime $\alpha_n=\pm\lambda_n$ (for the relevant transport bands) is realized [see the out-of-plane TAMR in case B of Table I]. In such a case, however, the out-of-plane TAMR with [001] as the reference axis should remain finite.

C. (111) MTJs with axes $\hat{x}\|[11\bar{2}]$, $\hat{y}\|[\bar{1}10]$, and $\hat{z}\|[111]$

The symmetry corresponding to the zinc-blende barrier grown in the [111] direction is given by the C_{3v} point group. In such a case the BIA-like SOC in the linear in $\mathbf{k}_\|$ approximation has the same form as the Bychkov-Rashba SOC [see Eq. (13)]. Therefore, the SIA due to the presence of interfaces does not lower the symmetry and the total SOC including both SIA-like and BIA-like terms reduces to the simple form[23]

$$H_{\text{SO}}=(\alpha_n+\gamma_n)(k_x\sigma_y-k_y\sigma_x), \tag{21}$$

where α_n and γ_n are the parameters characterizing the strengths of the SIA-like and BIA-like SOCs, respectively.

After computing the anisotropic part of the conductance we obtain

$$G^{(2)}_{\text{aniso}} = \frac{g_0 \sin^2 \theta}{8\pi^2} \sum_n c_n(\alpha_n + \gamma_n)^2. \tag{22}$$

This relation leads to the TAMR coefficients given in Table I for the case C.

In the present case the prediction of a vanishing in-plane TAMR is remarkable. We have checked that even if the cubic in k terms are included in the SOC field, the in-plane TAMR still vanishes. This could be used for experimentally exploring the origin of the TAMR. If a suppression of the in-plane TAMR is experimentally observed in (111) MTJs, it will be a strong indication that indeed the mechanism behind the TAMR is the SIA-like and/or the BIA-like SOCs. On the contrary, if no suppression of the in-plane TAMR is observed, the role of these spin-orbit interactions as the origin of the TAMR can be questioned.

Another interesting issue is the possibility of reaching the condition $\alpha_n = -\gamma_n$ (for the bands relevant to transport), which leads to a vanishing out-of-plane TAMR (if only the linear in k terms in the SOC field are relevant), in addition to the above-discussed suppression of the TAMR in the in-plane configuration.

D. Uniaxial strain in (001) MTJs with axes $\hat{\mathbf{x}}\|[100]$, $\hat{\mathbf{y}}\|[010]$, and $\hat{\mathbf{z}}\|[001]$

In our previous analysis we have disregarded the effects of the strain-induced SOC, which could be relevant for structures whose constituent materials have a sizable mismatch in their lattice constants. For a (001) MTJ, the SOC induced by strain is, in general, given by[30]

$$\begin{aligned} H_{\text{SO}} = \alpha_n[(u_{zx}k_z - u_{xy}k_y)\sigma_x + (u_{xy}k_x - u_{yz}k_z)\sigma_y \\ + (u_{yz}k_y - u_{zx}k_x)\sigma_z] + \gamma_n[k_x(u_{yy} - u_{zz})\sigma_x \\ + k_y(u_{zz} - u_{xx})\sigma_y + k_z(u_{xx} - u_{yy})\sigma_z], \end{aligned} \tag{23}$$

where u_{ij} are the components of the strain tensor and α_n and γ_n are material parameters. The SOC in Eq. (23) is quite rich and suggests the possibility of engineering the strain (see, for example, Ref. 31) in order to manipulate the behavior of the TAMR. Here we do not consider all the possibilities but focus, for the sake of illustration, on the case of an in-plane uniaxial strain such that the only nonvanishing components of the strain tensor are $u_{xx}=u_{yy} \neq u_{xy}=u_{yx}$. The existence of a similar strain was initially assumed for explaining TAMR experiments in (Ga,Mn)As/AlOx/Au MTJs.[1,3] For the in-plane uniaxial strain Eq. (23) reduces to

$$H_{\text{SO}} = \eta_n(k_x\sigma_y - k_y\sigma_x) + \mu_n(k_x\sigma_x - k_y\sigma_y), \tag{24}$$

where we have introduced the strain-renormalized SIA and BIA parameters $\eta_n = \alpha_n u_{xy}$ and $\mu_n = \gamma_n u_{xx}$, respectively. The corresponding anisotropic contribution to the conductance is then given by

$$G^{(2)}_{\text{aniso}} = \frac{g_0 \sin^2 \theta}{8\pi^2} \sum_n c_n[(\eta_n^2 + \mu_n^2) + 2\eta_n\mu_n \sin(2\phi)]. \tag{25}$$

We note that Eq. (24) has the form of interfering Bychkov-Rashba and Dresselhaus SOCs in (001) structures with $\hat{\mathbf{x}}\|[100]$.[12,23] Therefore, Eqs. (16) and (25) are similar. The angle ϕ in Eq. (16) is measured with respect to the crystallographic direction [110] while in Eq. (25) it is defined with respect to the [100] axis. Thus, by making the transformation $\phi \to \phi + \pi/4$ in Eq. (25) one recovers a relation similar to Eq. (16). Consequently, assuming the direction [110] as the reference axis for measuring the magnetization direction the results for the in-plane and out-of-plane TAMR coefficients in (001) MTJs with in-plane uniaxial strain [see case D in Table I] are essentially the same as in the case discussed in A but with renormalized spin-orbit parameters, which now account for the strain effects.

E. Other possible effects on the TAMR

In our investigation we have assumed specific well-known forms for the SOC field. For some systems, however, the form of the SOC field may not be *a priori* known. In such a case one could use Eqs. (8)–(10) (which are general) and contrast them with complementary TAMR measurements in both the in-plane and out-of-plane configurations in order to deduce the symmetry properties of the SOC fields.

All the calculated TAMR coefficients, if not zero, show a twofold symmetry in the (θ, ϕ) space, which is the symmetry that has been observed in the experiments.[4,5,9,11,17] Our results are valid up to the second order in the SOC field. In particular, our predictions for vanishing TAMR under certain conditions may change when higher orders in the SOC field become relevant. The next higher-order contributions in the expansion in Eq. (4) which do not vanish after averaging are those containing the fourth order in the SOC field terms and terms of the fourth order in the cosine directions of $\hat{\mathbf{m}}$, which describe the fourfold symmetry inherent to the involved bulk ferromagnet. These fourth-order terms lead to fourfold symmetric corrections to the TAMR, which may be finite even for (001) MTJs with centrosymmetric barriers for which the second-order in-plane TAMR calculated here vanishes. Although the twofold character of the TAMR is, in general unchanged by these corrections, they may influence the shape of its angular dependence. Additionally, in some heterostructures the SOC field itself may become magnetization dependent due to changes in the electronic band structure when the magnetization orientation is varied. This effect, which is not included in our approximation, may also influence both the size and the polar shape of the TAMR. Thus, for the kind of systems considered here (see Table I) any deviation from the 8-*like* polar shape of the TAMR [see, for example, Fig. 2 in Ref. 5] is interpreted in our theory as a manifestation of higher-order contributions (in $\mathbf{k}_\|$ and/or $\hat{\mathbf{m}}$) and/or strain effects.[32] Deviations from the 8-*like* polar shape of the TAMR have been experimentally observed.[9,11] In fact, it has been shown that these deviations may appear by increasing the bias voltage,[11] which within the present approach can be seen as an indication of higher order in the SOC field terms turning relevant at sufficiently high bias.

In all the above discussions small magnetic fields with negligible orbital effects were assumed. It has recently been observed in Fe/GaAs/Au MTJs that for high magnetic fields the orbital effects do influence the in-plane TAMR.[33] A version of the phenomenological model presented here, which incorporates the orbital effects, has recently been developed to qualitatively explain the magnetic field dependence of the in-plane TAMR experimentally observed in (001) Fe/GaAs/Au MTJs.[33]

IV. SUMMARY

We formulated a theoretical model in which the way the TAMR depends on the magnetization orientation of the ferromagnetic electrode in MTJs is determined by the specific form and symmetry properties of the interface-induced SOC field. By using the proposed model, we deduced the angular dependence of the TAMR for various systems in dependence of their symmetries under spatial inversion and their growth directions. The effects of in-plane uniaxial strain were also investigated.

ACKNOWLEDGMENTS

We thank S. D. Ganichev, S. A. Tarasenko, and D. Weiss for useful discussions. This work was supported by the Deutsche Forschungsgemeinschaft via Grant No. SFB 689.

[1] C. Gould, C. Rüster, T. Jungwirth, E. Girgis, G. M. Schott, R. Giraud, K. Brunner, G. Schmidt, and L. W. Molenkamp, Phys. Rev. Lett. **93**, 117203 (2004).
[2] L. Brey, C. Tejedor, and J. Fernández-Rossier, Appl. Phys. Lett. **85**, 1996 (2004).
[3] C. Rüster, C. Gould, T. Jungwirth, J. Sinova, G. M. Schott, R. Giraud, K. Brunner, G. Schmidt, and L. W. Molenkamp, Phys. Rev. Lett. **94**, 027203 (2005).
[4] H. Saito, S. Yuasa, and K. Ando, Phys. Rev. Lett. **95**, 086604 (2005).
[5] J. Moser, A. Matos-Abiague, D. Schuh, W. Wegscheider, J. Fabian, and D. Weiss, Phys. Rev. Lett. **99**, 056601 (2007).
[6] A. D. Giddings, M. N. Khalid, T. Jungwirth, J. Wunderlich, S. Yasin, R. P. Campion, K. W. Edmonds, J. Sinova, K. Ito, K.-Y. Wang, D. Williams, B. L. Gallagher, and C. T. Foxon, Phys. Rev. Lett. **94**, 127202 (2005).
[7] A. B. Shick, F. Máca, J. Mašek, and T. Jungwirth, Phys. Rev. B **73**, 024418 (2006).
[8] M. Elsen, H. Jaffrès, R. Mattana, M. Tran, J.-M. George, A. Miard, and A. Lemaître, Phys. Rev. Lett. **99**, 127203 (2007).
[9] M. Ciorga, M. Schlapps, A. Einwanger, S. Geißler, J. Sadowski, W. Wegscheider, and D. Weiss, New. J. Phys. **9**, 351 (2007).
[10] A. N. Chantis, K. D. Belashchenko, E. Y. Tsymbal, and M. van Schilfgaarde, Phys. Rev. Lett. **98**, 046601 (2007).
[11] L. Gao, X. Jiang, S. H. Yang, J. D. Burton, E. Y. Tsymbal, and S. S. P. Parkin, Phys. Rev. Lett. **99**, 226602 (2007).
[12] J. Fabian, A. Matos-Abiague, C. Ertler, P. Stano, and I. Žutić, Acta Phys. Slov. **57**, 565 (2007).
[13] P. Sankowski, P. Kacman, J. A. Majewski, and T. Dietl, Phys. Rev. B **75**, 045306 (2007).
[14] D. Jacob, J. Fernández-Rossier, and J. J. Palacios, Phys. Rev. B **77**, 165412 (2008).
[15] M. N. Khan, J. Henk, and P. Bruno, J. Phys.: Condens. Matter **20**, 155208 (2008).
[16] R. S. Liu, L. Michalak, C. M. Canali, L. Samuelson, and H. Pettersson, Nano Lett. **8**, 848 (2008).
[17] B. G. Park, J. Wunderlich, D. A. Williams, S. J. Joo, K. Y. Jung, K. H. Shin, K. Olejník, A. B. Shick, and T. Jungwirth, Phys. Rev. Lett. **100**, 087204 (2008).
[18] A. B. Shick, F. Máca, M. Ondráček, O. N. Mryasov, and T. Jungwirth, Phys. Rev. B **78**, 054413 (2008).
[19] A. Matos-Abiague and J. Fabian, Phys. Rev. B **79**, 155303 (2009).
[20] M. Gmitra, A. Matos-Abiague, C. Ambrosch-Draxl, and J. Fabian (unpublished).
[21] Y. A. Bychkov and E. I. Rashba, J. Phys. C **17**, 6039 (1984).
[22] G. L. Bir and G. E. Pikus, *Symmetry and Strain-Induced Effects in Semiconductors*, 1st ed. (Wiley, New York, 1974).
[23] X. Cartoixà, L.-W. Wang, D. Z.-Y. Ting, and Y.-C. Chang, Phys. Rev. B **73**, 205341 (2006).
[24] G. Dresselhaus, Phys. Rev. **100**, 580 (1955).
[25] M. I. Dyakonov and V. Y. Kachorovskii, Sov. Phys. Semicond. **20**, 110 (1986).
[26] If the values of α_n and γ_n are substituted by their respective averages $\tilde{\alpha}$ and $\tilde{\gamma}$, the relation obtained for $\text{TAMR}^{\text{in}}_{[110]}$ (see case A in Table I) reduces to the expressions reported in Refs. 12 and 19.
[27] Here a finite TAMR is still possible if higher-order terms in the SOC field are relevant.
[28] Note that for the out-of-plane configuration changing the reference axis implies changing the plane in which the magnetization is rotated (see Fig. 1).
[29] H. Diehl, V. A. Shalygin, V. V. Bel'kov, C. Hoffmann, S. N. Danilov, T. Herrle, S. A. Tarasenko, D. Schuh, C. Gerl, W. Wegscheider, W. Prettl, and S. D. Ganichev, New J. Phys. **9**, 349 (2007).
[30] G. E. Pikus and A. N. Titkov, in *Optical Orientation, Modern Problems in Condensed Matter Science*, edited by F. Meier and B. P. Zakharchenya (North-Holland, Amsterdam, 1984), Vol. 8, p. 73.
[31] E. De Ranieri, A. W. Rushforth, K. Výborný, U. Rana, E. Ahmad, R. P. Campion, C. T. Foxon, B. L. Gallagher, A. C. Irvine, J. Wunderlich, and T. Jungwirth, New J. Phys. **10**, 065003 (2008).
[32] For the in-plane uniaxial strain considered here [see Eq. (24)] the angular dependence of the in-plane TAMR deviates from the 8-like polar shape only if higher than second-order terms in the SOC field become relevant. However, for other kinds of strains different shapes may appear already at the second order in the SOC field.
[33] M. Wimmer, M. Lobenhofer, A. Matos-Abiague, D. Schuh, W. Wegscheider, J. Fabian, D. Weiss, and K. Richter, arXiv:0904.3017 (unpublished).